Stress Analysis Of An Aerodynamically Loaded Structure Under Supersonic Conditions

G. Chen, K. Walker, G. Swanton and S. Hill
Air Vehicles Division, Platform Sciences Laboratory
Defence Science and Technology Organization
P O Box 4331, Melbourne, Australia 3001

ABSTRACT This paper presents a stress analysis carried out in order to understand the effect of engine intake aerodynamic loads on the F-111 FS496 former and surrounding intake structure. In the cases investigated, the air pressure distributions were known, so the air pressure was applied directly to the intake nacelle wall. A sensitivity study was subsequently carried out to compare a real pressure distribution and different functions representing the pressure distribution. It was concluded that the results were not greatly affected by the different functions.

1 INTRODUCTION

Cracking of the fuselage station 496 (FS496) nacelle formers on the F-111 aircraft has been a problem for both the Royal Australian Air Force (RAAF) and the United States Air Force (USAF) [Ignjatovic, 2003]. The FS496 nacelle former is primary structure and its failure is likely to result in catastrophic loss of the aircraft. There has been a lack of general understanding of cracking issues for the FS496 nacelle former. An investigation of the causes of cracking of the nacelle former is therefore considered important.

Being a high strength D6ac welded steel forging situated near the entrance to each engine intake, as shown in Fig. 1, the FS496 nacelle former not only redistributes body loads from the wing carry –through box (WCTB) to the fuselage, but also provides support for the forward intake structure, stabilisation of surrounding longerons and structural panels, and transmission of air pressure loads from the nacelle wall panels to the wing carry –through box.

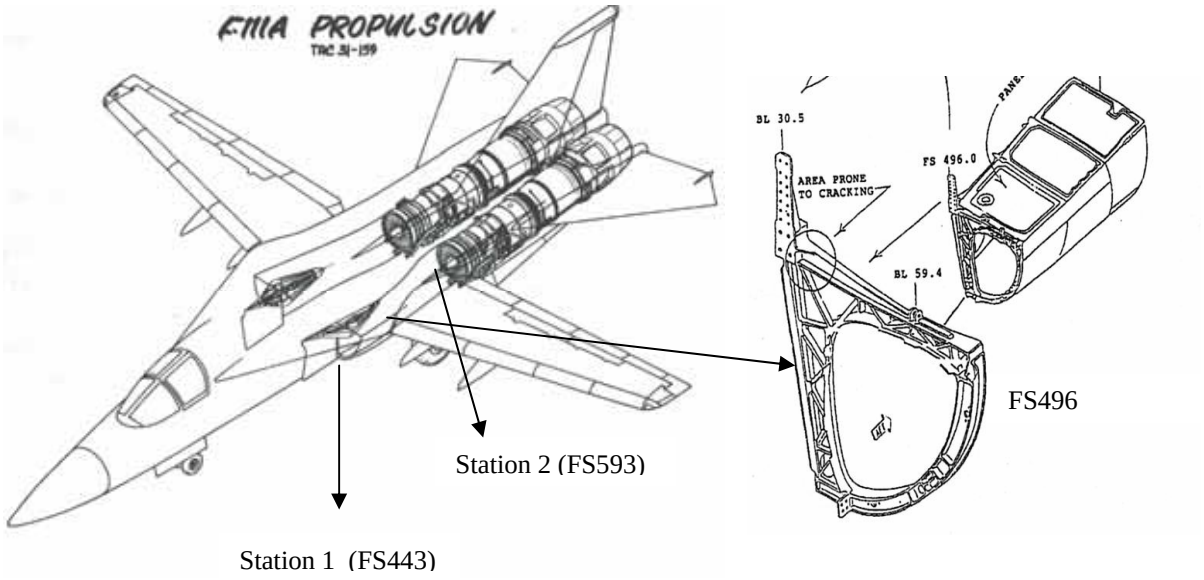

Figure 1. F-111 Propulsion, Nacelle Former, and Intake Structure.

In order to understand the effects of aerodynamic intake loads on the FS496 former and surrounding intake structure, a stress analysis was initially carried out. In the cases being studied,

the air pressure distributions were known, so these pressures were applied directly to the intake nacelle wall. Secondly, a sensitivity study was subsequently carried out to compare a real pressure distribution with pressure distributions represented by different functions.

2 ENGINE CHARACTERISTICS

For a jet engine [Cox, 1981], there are five major turbo-machinery components; air intake, compressor, combustion chamber, turbine and exhaust section. Each of these has a unique contribution to the generation of thrust. The intake provides the appropriate amount of airflow required by the engine. The airflow must be stable when leaving the intake section, not only during all phases of flight, but also on the ground with the aircraft at rest and the engine demanding maximum thrust prior to take off. The entrance of the air intake is defined as Station 1, and Station 2 defines the entrance to the compressor face or the outlet of the air intake shown in Figure 2. Although this component may look simple in appearance, it presents a number of fluid flow and mechanical problems [Hueneche, 2001]. The air intake is essentially a fluid flow duct whose task is to process the airflow in a way that ensures the engine functions properly to generate thrust. In a supersonic aircraft, the air intake can become an extremely complex device requiring enormous effort to properly control the airflow to the engine.

When a certain compressor face Mach number is commanded by setting the throttle to the desired position, the inlet adjusts airflow itself, either by increasing the spillage or reducing it to achieve either a lower or higher compressor face Mach number. The complexity of the air intake obviously makes intake design and calculation an onerous task [Hueneche, 2001]. As the flow follows the contour of the nacelle, excessive velocity can develop which may even attain low supersonic speeds. This will also cause a zone of low pressure around the intake circumference, leading to the exertion of an aerodynamic force with a component acting in the direction of engine thrust.

3 FINITE ELEMENT MODELLING OF F-111 AND FS496

A coarse grid finite element model (CG FEM) of the F-111C aircraft structure has been developed to accurately predict the internal load distribution under specified external loads [Mann et al., 2000], including the special case of the cold proof load test (CPLT)[1]. A diagram of the model is shown in Figure 2. The nacelle structure between Station 1 and Station 2 is of particular interest here.

3.1 FE Mesh

The FEM shown in Figure 2(a) for the F-111 was imported in MSC Patran [Patran, 2001]. The geometry, the finite element mesh, properties, materials and groups were also defined using Patran. The “group” function of Patran is utilised to separate the numerous parts and assemblies. All finite element linear elastic analyses were performed by MSC Nastran [Nastran, 2001]. All analysis results were post-processed by Patran.

[1] Cold Proof Load Testing (CPLT) is a periodic proof load testing program performed in a special facility on the F-111 structure to confirm the absence of any flaws in D6ac steel above a very small size. It then clears that structure for a further period of safe flight. In CPLT, the aircraft is cooled to -40^{o}F to embrittle the D6ac steel structure, and then loads appropriate to (g is an acceleration) –2.4g and +7.33g at 56^{o} wing sweep angle and –3.0g and 7.33g at 26^{o} wing sweep angle are applied.

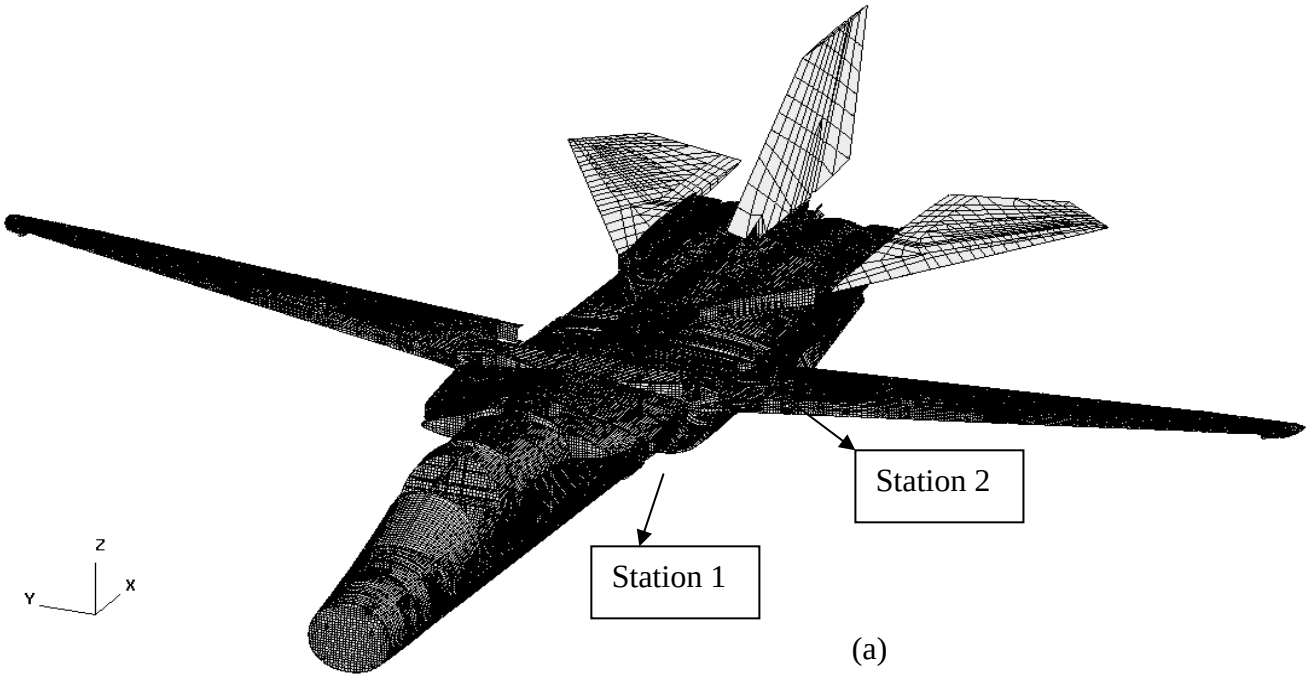

(a)

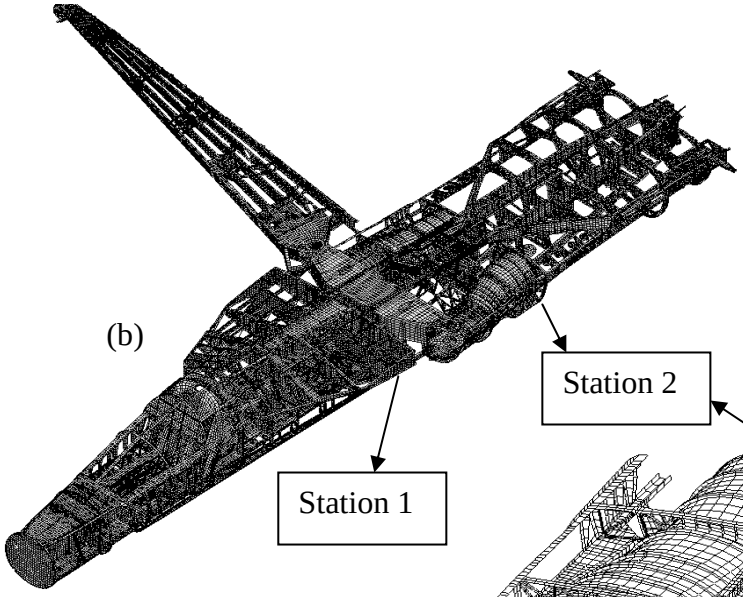

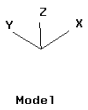

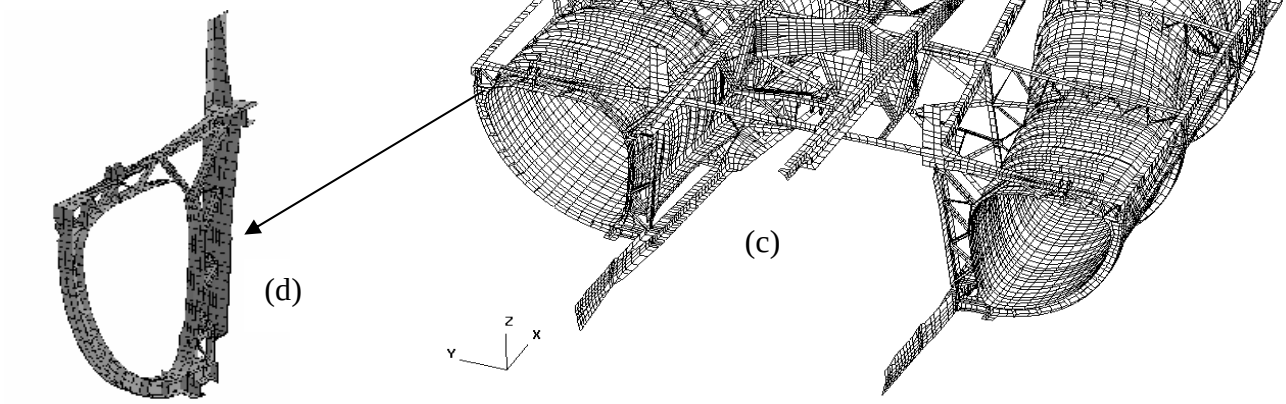

Figure 2 FE mesh (a) total mesh of F-111, (b) mesh details of one part of F-111, (c) mesh details of intake structure and (d) mesh details of FS496 Former

Figure 2(a) shows basic meshes of the FE model for the F-111 with more details shown in Figure 2(b). It contains meshes for structural components such as longerons, bulkheads, skins, panels and other miscellaneous structures, including a rudimentary representation of the vertical and horizontal tails to ensure proper load introduction to the aft fuselage. A dummy structure with reaction points at the correct geometrical locations was developed for items such as the landing gear and the wing control surfaces. Any other structure that was not deemed to be structurally significant (clips, small brackets, etc.) was not included in the F-111C CG FEM. Imperial British System (IBS) of units pound-force (lb), inch (in), second (s) and degree Fahrenheit (°F) was used in this model, the results have been transferred into SI System here.

Predominantly, quadrilateral and triangular shell elements were used along with rod, beam and three-dimensional solid elements. In general, the FEM representation of the aircraft joints is made with overlapping elements and common grid points. Joints that only transfer loads in certain degrees of freedom are modelled by spring elements possessing the corresponding degrees of freedom. The F-111C CG FEM consists of approximately 315,500 grid points and 393,600 elements, resulting in approximately 1,870,000 degrees of freedom.

The mesh detail of the nacelle tunnel assemblies is shown in Figure 2(c), which contains all primary and secondary structure for this region with the exception of the main landing gear doors and the nacelle inlet spike, since they do not carry any significant load into the surrounding structure. The nacelle assembly is connected to the surrounding structure via the fore-aft running longerons and shear panels, as well as the FS496 former to the wing carry-through box connection. The mesh details of FS496 former are shown in Figure 2(d). The wing pivot is accounted for by a pin connection on the wing carry-through box, which reacts wing bending and torsion by a couple mechanism. Vertical shear loads are reacted via the shear receptacle that is located on the outboard bulkhead of the wing carry-through box, and the shear ring, which is bolted to the inboard section of the wing pivot fitting. The solid elements are used to transfer shear loads. The beam and spring elements are used to represent the wing pin connection to transfer loads from the wing to the wing carry-through box. On the outer of the radial beams, the spring elements are placed to react the primary axial load. At the free end of beams, additional springs have also been placed to prevent numerical singularity for the joint in the vertical and theta (rotation about the pin axis) direction. The grid points associated with the spring elements have been placed in a cylindrical coordinate system with the origin at the wing pivot point to enable the correct load transfer. The wings can be placed at a number of different wing sweep angles: 16, 26 and 56 degrees. In the case concerned for Mach number 1.37, the wing sweep angle is 26 degrees.

3.2 Material properties

The nacelle former assembly is manufactured from D6ac Steel, while another five different types of material were utilised in the F-111C CG FEM. A summary of the materials [Military Handbook, 2001] used is listed in Table 1. All the materials were simulated with an isotropic MSC.NASTRAN MAT1 card in Nastran by using materials constants as required.

Table 1. Material data for F-111C CG FEM

Material Name	Young's Modulus (Pa)	Poisons ratio
D6AC Steel	2.00E+11	0.32
Aluminum	7.10E+10	0.33
Titanium	1.13E+11	0.31
Stainless Steel	2.00E+11	0.28
Fiberglass	2.55E+10	0.1
Glass	6.89E+10	0.22

3.3 Loads

Two types of loading were applied – inertial and aerodynamic load. Since all structural parts were modelled without mass properties, the inertial load needed to be determined. For the external aircraft surface aerodynamic loads, Platform Sciences Laboratory (PSL) constructed a CFD model of the F-111C aircraft for the Euler CFD code RAMPANT, which was then used to determine the

pressures over the entire aircraft for a wide variety of flight conditions. Specifically, the CFD data were computed for a Mach range of 0.2 to 1.4, angle of attack -4^o to 10^o and wing sweeps of 16^o, 26^o, 45^o, 54^o and 72^o. For the F-111C wing, these pressure distributions were integrated over the panel areas to determine shear, moment, torsion (V, M, T) distributions for a given flight condition through the use of a Fortran procedure called "AeroDatabase"; written by PSL. Flight condition parameters are used for this procedure.

4 FE ANALYSIS AND SENSITIVITY STUDY

The FE analysis was conducted without any consideration of variation in temperature. The initial stage in determining in-flight loads was to determine the mass distribution of the F-111C aircraft. The mass distribution is required to determine the internal inertia forces on the frame of the aircraft during a manoeuvre due to linear and angular accelerations. The balance of mass was assessed according to the methods from [Mann et al., 2000].

The steady pressure data along the intake wall for the supersonic conditions came from [Evans, 1971]. From this source, it could be seen that the steady pressure loads along the intake nacelle wall reached a peak at Mach number 1.37, thus the analysis for this particular case is documented here. The solid curve in Figure 3 shows the steady pressure distribution over the intake nacelle wall at Mach number 1.37, just before an engine stall, with the steady pressure at Station 1 $p_1=40.00$ psi and the steady pressure at Station 2 $p_2=42.85$ psi. The corresponding external aircraft surface aero loads were determined from CFD. The closest available flight condition parameters from the CFD were for M=1.4 at sea level, and these were used to obtain pressure data for the external surfaces of the aircraft according to [Morgan et al., 1997]. Then the pressure distribution was integrated over the panel areas to compute wing VMT distributions. These VMT distributions are used to load the F-111C CG FEM. The wing VMT distribution is interpolated from the available CFD VMT distributions. The VMT data are passed back as an array of VMT loads with respect to a given span wise location. The above mentioned external aircraft surface aero loads do not include the air pressure in the intake nacelle. In addition to the external aircraft surface aero loads, the pressure loads within the intake were loaded here directly to the inner surface panels of the intake nacelle wall by using panel pressure loads for Nastran load input decks.

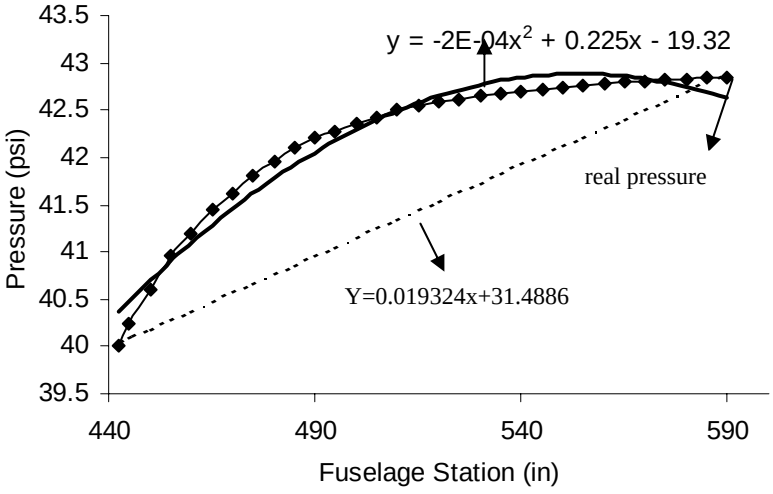

Figure 3. The pressure distribution within the intake

The FE results in the form of contour plots are shown in Figure 4. Figure 4(a) shows von Mises stresses for FS496 with only the external aircraft surface aero loads (CFD data only), with the stress for the critical location of FS496 former (lower inboard forward flange area) being 26.3 MPa. Figure 4(b) shows von Mises stress for FS496 with both the external aircraft surface aero loads and the intake steady pressure loads just before an engine stall at M=1.37 (both CFD data and data from [Evans, 1971]), with the stress at the critical location being 73.8 MPa. Comparing Figures 4(a) and 4(b), there is a 180% difference in the von Mises stress at this critical location between the two

cases, showing the effect of aerodynamic intake loads on the FS496 former. If the intake peak stall pressure due to an engine stall at M=1.37 is loaded on this model together with aero loads, the von Mises stress at this critical location reaches 105 MPa. The pattern of the contour plot showing the von Mises stress and the location of the peak stress for this engine stall case is the same as Figure 4(b). The change of peak stress alters the critical crack size, hence affecting the estimation of the fatigue life in a future crack growth analysis.

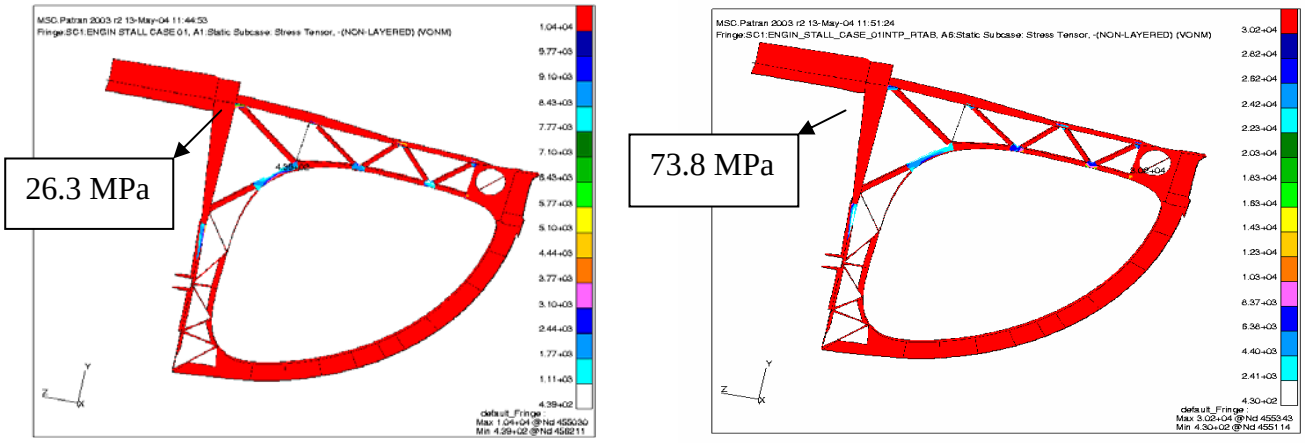

(a) **(b)**

Figure 4 FE results of von Mises stresses for FS496, (a) with only the aero loads; and (b) with both the aero loads and the intake pressure loads.

In order to estimate the pressure distribution for the cases where the pressure distribution along the intake section are not known, which is documented in [Chen, G. et al 2004], a sensitivity study was carried out to compare a real pressure distribution and different functions representing the pressure distribution for this region. For example, with "x" representing the fuselage station and "y" representing the pressure (in psi), a second order polynomial function obtained by curve fitting (with 96.87% deviation) can be used to represent the real pressure distribution, between Stations 1 and 2, which can be expressed as:

$$y = -0.0002x^2 + 0.225x - 19.32 \qquad (1)$$

The intake aerodynamic pressure distribution represented by Eq (1) was directly loaded to the surface panel of the intake. The results of the von Mises stress are shown using a contour plot in Figure 5(a).

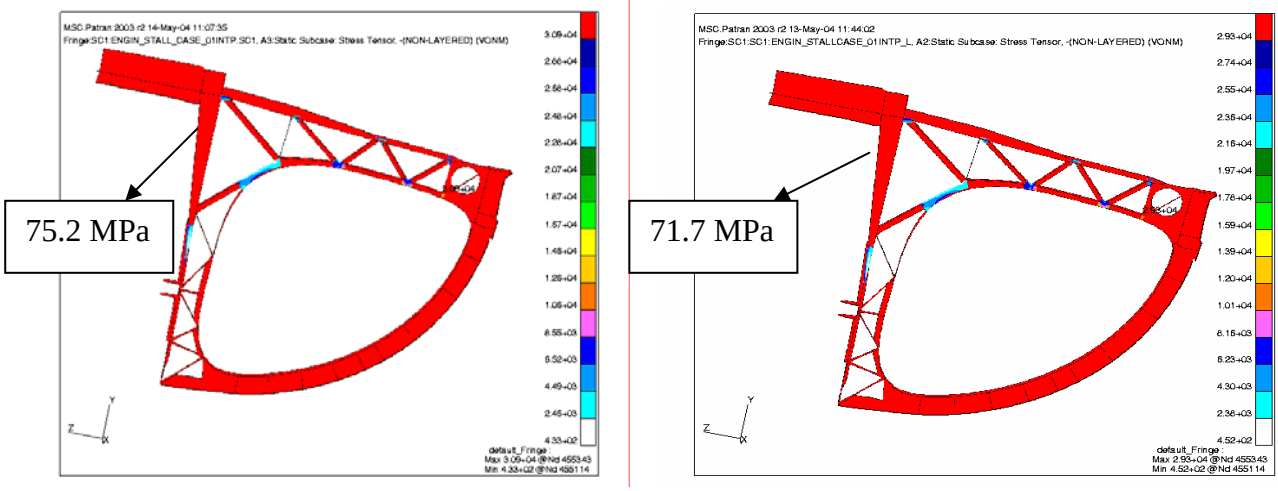

(a) (b)

Figure 5 FE results of von Mises for FS496, with intake pressure distribution being represented by (a) second order polynomial function Eq (1), and (b) a linear equation, Eq (2).

Keeping p_1=*2.76E+05* pa and p_2=*2.95E+05* pa, a linear function was also determined to represent the pressure distribution between Stations 1 and 2, which can be expressed as:

$$y = 0.019324x + 31.4886 \quad (2)$$

Applying the pressure distribution represented by Eq (2), the FE results of the von Mises stress is shown in Figure 5(b).

Comparing Figures 4(b), 5(a) and 5(b), the pattern of the contours are virtually the same, with little difference in von Mises stress at the same critical location, eg: 2.88% difference for pressure distribution being represented by the linear function. The same result can be observed for FE results of other stress components in the FS496 former. Therefore, it is concluded that the results were not greatly affected by the different functions being used to represent pressure within the intake. For its simplicity, Eq (1) is recommended for future use.

5 CONCLUSIONS

1 Finite element based analyses using Nastran were performed to calculate the stresses at FS496, giving consideration to air pressure loads along the intake nacelle wall.

2 These results were further compared to the results obtained without this consideration. The comparison shows differences for the critical location of the FS496 former (lower inboard forward flange area), eg: (a) 180% difference for the von Mises stress at Mach number 1.37, showing the effect of aerodynamic intake loads on FS496 former and surrounding intake structure; (b) 300% difference for von Mises stress at this location for the engine stall case at Mach number 1.37. If it is seen as the worst case condition, this peak stress would alter the existing critical crack size, which does not consider the intake pressure loads, and hence affect the estimation of the fatigue life. It is also noted here that the absolute values of the von Mises stresses for the critical location for the case investigated are not significant high for D6ac steel as the FE model is based on the coarse grid meshes which does not consider the stress concentration.

3 A sensitivity study was subsequently carried out with both a real pressure distribution and different functions representing the pressure distribution. It was concluded that the results were not greatly affected by the different functions.

ACKNOWLEDGEMENT The input from Dr. Norman Freund from Aerostructures Pty Ltd is highly appreciated.

REFERENCES:

Chen, G, Walker, K, Swanton G and Hill, S: An Envelope Method for Stress Analysis of the F-111 Fuselage Station 496 (FS496) Nacelle Former under Subsonic Conditions, SIF 2004 paper (2004)

Cox, HR Sir: *Gas Turbine Principles And Practice*, Pergamon Press, (1981)

Evans P J: Magnitude and Distribution of Air Induction System Design Loads for F-111 Series Airplane Equipped with Triple Plow and Triple Plow II Inlet., General Dynamics. FZS-12-289 (1971)

Hueneche, K: *Jet Engines Fundamentals of Theory*, Design and Operation, Airlife, England. (2002)

Ignjatovic, M: Investigation of the F111 FS496 Region Cracking Issues and Reviewed DADTA for Relevant DADTA Items – Part 1. (2003)

Mann, N, Jones, T F and Hill, S: F-111C Airplane Grid Finite Element Model for Royal Australian Air Force. Lockheed Martin Corperation, FZS-12-38001 (2000)

Military Handbook 5H *Metallic Materials and Elements for Aerospace Vehicle Structures*, December (1998)

MSC/Nastran, *User Manual*, MSC Software. (2001)

MSC/ Patran *User Manual*, Version 9.0

Morgan, J, Rungsiyaphornrat, S and Sherman, D J F-111C Wing Damage Enhancement Test: Aerodynamic Loads from CFD Analysis, *DSTO-DP-0441*, Defence Science and Technology Organisation, (1997)